RESEARCH REPORT

VTT-R-00494-17

Validation and verification of the photon transport capabilities in Serpent 2.1.27

Authors: V. Valtavirta, R. Tuominen

Confidentiality: Public

Contents

1. Introduction

Computational models for atomic photon physics were recently developed and implemented in Serpent 2 as the Master's thesis work of T. Kaltiaisenaho[1]. The new photon calculation capabilities extend the applications of Serpent 2 especially in the direction of radiation shielding and photon dose rate calculations. In order to apply these new capabilities to real world problems, the capabilities need to be validated against experimental data in order to obtain a quantitative estimate for the uncertainties included in the computational model.

This report details the beginning of the validation and verification of the photon physics in Serpent 2. Potential experiments for the validation of the photon dose rate calculation by Serpent were identified first: Two experiments used for the photon transport validation of MCNP[2] were chosen to be modeled in this first phase of validation. The suite of SINBAD shielding benchmark experiments[3] was also reviewed and the potential of each experiment in the suite for the validation purposes was estimated.

Section 2 and 3 will describe the modeling of the Kansas skyshine experiment[4] as well as the Hupmobile thermoluminecent dosimeter experiments[5, 6] with Serpent 2.1.27 and MCNP6. In the former experiment, experimental data was available for comparison, whereas in the latter experiment the comparison is done between Serpent 2 and MCNP6. All of the simulations were conducted using the photoatomic interaction data contained in the mcplib84 photon physics library distributed with MCNP6. Serpent also used the standard set of additional data required for the advanced photon physics models of Serpent that are described in Ref. [1].

Section 4 describes the experiments of the SINBAD database that are of particular interest for future photon physics validation of Serpent 2. From each relevant experiment, the measured quantities alongside with additional important information concerning the future modeling of the experiments are listed.

2. Gamma-ray skyshine experiments

2.1 Problem description

Reference [4] presents three different skyshine experiments conducted at a shielding research facility in Kansas in 1980. The first of the three experiments was used in the validation of the photon physics routines of MCNP as described in [2]. The experiments measured the energy spectrum and exposure rates of photons emitted by ^{60}Co on an open field at distances up to 700 m from the source.

2.2 Experimental arrangement

This description is based on Ref. [4]. In the experiments a point ^{60}Co gamma source was placed on the axis of an approximately annular (in reality 12-sided) concrete silo. The source was located 1.98 m above the base of the silo. The silo had a height of 2.29 m, an inner diameter of 2.50 m and an outer diameter of 4.35 m. In the first experiment the top of the silo was open and wedge shaped concrete blocks backed by lead blocks were placed around the top of the silo wall so that uncollided photons from the source would exit the top of the silo in a 150.5° vertical cone. In the second and third experiment, no wedge shaped collimator blocks were used. Instead, the top of the silo was covered with a concrete roof with a thickness of either 21 cm (experiment 2) or 42.8 cm (experiment 3).

Photon detectors were placed at various distances between 30 m and 700 m from the source. Two types of detectors were used in the experiment. A NaI(Tl) detector located 2.2 m above the ground was used to measure gamma energy spectra and exposure rates. A 25.4 cm diameter spherical high pressure ion chamber (HPIC) located 1.0 m above ground was used for the exposure rate measurements only. The open field, where the experiments were conducted was not completely flat meaning that the maximum HPIC detector elevation relative to the source was 2.51 m and the average elevation was 1.39 m.

2.3 Serpent and MCNP models

2.3.1 Experiment 1: Unshielded 150.5° cone, basic input

The Serpent model for the first experiment was based on the MCNP model presented in Ref. [2], which also included an example MCNP input. The geometry was bounded by a 1 km sphere placed at the origin and a plane perpendicular to the z-axis at $z = -9.0$ cm slicing the sphere. The ground-air interface was represented by a plane at z = 0.0 cm. The volume enclosed by the two planes and the sphere was filled with soil. The MCNP model included in the validation report used a standard soil elemental composition with a density of 2.6 g/cm^3 as no soil composition or density was specified for the experiments. The same material composition was also used in all of the Serpent models.

The annular concrete silo was modelled as a region between two concentric cylinders centred at origin intersected by the xy-plane and another horizontal plane defining the top of the silo. The silo had a inner radius of 117.75 cm[1], an outer radius of 217.5 cm and a height of 229 cm. MCNP silo geometry is presented in Figure 1. In the MCNP model zero importance was set to the region containing the silo and the ground directly below the silo. Photons that entered

[1] The inner radius is smaller than that in the experimental model in order to create the 150.5° collimated photon cone without defining the wedge blocks in the geometry model.

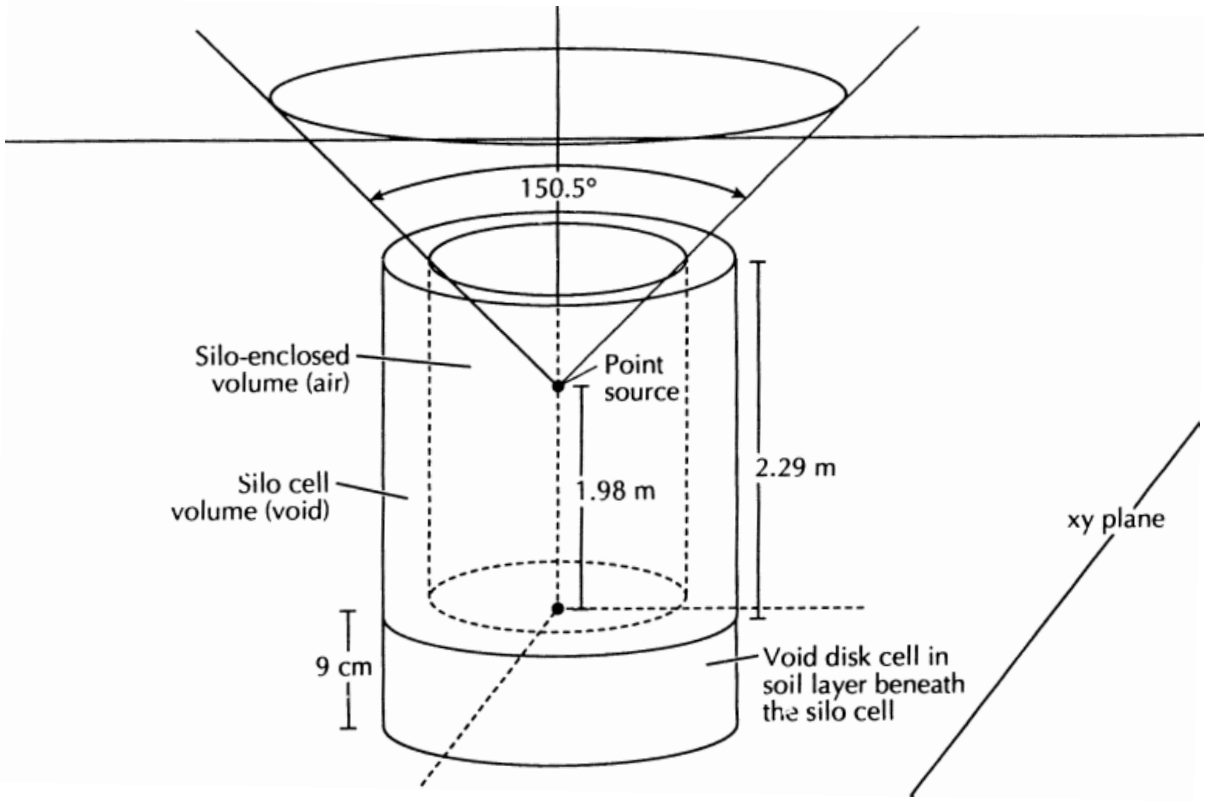

Figure 1. MCNP silo and source geometry (Source: [2]).

this region were terminated so there was no in-silo scattered component in the skyshine[2]. In the Serpent model the same region was defined as an outside region resulting in a similar termination of any photons hitting the silo walls. The volume enclosed by the silo and the volume outside the silo bounded by the XY-plane and the sphere were filled with air. Air density varied during the experiments and was taken in account during the post processing of the results. The calculation model used air with standard composition at 0.001124 g/cm^3.

The ^{60}Co gamma source was modelled as an isotropic point source which emitted 1.332 MeV and 1.173 MeV photons with equal probability. The source was placed at z = 1.98 m on the silo's axis. In the Serpent model source rate was set to 1 photon/s.

To model the exposure rates measured with the HPIC detectors eight concentric ring detectors centred at the origin were placed at z = 1.0 m and parallel to the XY-plane in the MCNP model. The radii of the ring detectors corresponded to the distances of the HPIC detectors from the source: 50 m, 100 m, and 200 m to 700 m at 100 m intervals. By modifying the flux estimate of each detector with an FM card, the energy deposited in unit volume per photon history MeV/(cm^3·history) was obtained.

In the Serpent model the exposure rate measurements were modelled with track-length detectors and response function -26, which is the macroscopic total energy deposition cross section. Each of the detectors was defined using a toroidal surface with a minor radius of 12.7 cm corresponding to the radius of the HPIC and a major radius corresponding to the distance from the source (e.g. 50 m). The output of the detectors was in units of J/history.

The MCNP model used a variance reduction technique based on assigning importances to the cells. In both Serpent and MCNP models a cut-off energy of 39.9 KeV was applied so no time was wasted following photons with energies below the detector response function in the

[2]This also ignores the photons that penetrate the vertical walls of the silo.

experiment. In the Serpent model delta-tracking threshold was set to zero so only surface-tracking was used as delta-tracking could have transported neutrons through the walls of the silo. It must be pointed out that this is an unconventional practice that was applied to for the sake of consistency with MCNP results. The use of delta-tracking may produce non-physical results if the outside region of the geometry is re-entrant. In these calculations the problem was avoided by switching delta-tracking off, but in general this practice is discouraged. Thick-target bremsstrahlung approximation (TTB) was set on in the Serpent model. In order to minimize the number of virtual collisions in the calculation, the minimum mean distance for the collision flux estimator (`set minxs`) was set to 1×10^6 cm.

2.3.2 Experiment 1: Unshielded 150.5° cone, realistic

The first input based on the reported MCNP model ignored the in-silo scattered photons as well as the photons that managed to penetrate the silo walls by terminating all photon histories that hit either the silo or the ground directly below the silo. Moreover, the concrete wedge blocks used to shape the gamma source were not included in the model and the directionality of the source cone was ensured by modifying the inner radius of the silo walls instead. The reason for these choices is not entirely clear, although they may be based on the fact that no information is given on the composition of the concrete making up the silo walls and the wedge blocks. Moreover the exact geometry of the wedge blocks is unknown.

Test calculations indicated that the in-silo scattered component as well as the silo wall penetrating component of the gamma source were not insignificant. Based on this, a decision was made to also create a more realistic geometry model in which the silo walls were modelled as concrete and the photons hitting the silo or the ground directly below the silo were not terminated. The composition of the silo walls was chosen to be composition 86 (Concrete, Los Alamos (MCNP)) from the Compendium of Material Composition Data for Radiation Transport Modeling [7] using the mass density given for the concrete roof tiles. The compositions listed in the compendium are included in Serpent 2 and can be listed from the command line with `./sss2 -comp list`.

The differences between this geometry model and the one described in the previous section are as follows:

- The silo walls are modelled as concrete instead of an infinitely absorbing material.
- The ground below the silo was modelled as soil instead of an infinitely absorbing material.
- The silo wall inner radius was set to 125 cm (as described in [4]) rather than to 117.75 cm.
- Concrete wedges were added on top of the silo walls to create a 150.5° aperture for the source photons.

An XZ-cut of the silo geometry is shown in Fig. 2 for the two geometry models for the first experiment.

2.3.3 Experiment 2: 21 cm thick concrete roof

For the second experiment, the geometry model was based on the realistic input for the first experiment: The wedge blocks were removed from the silo walls and a 21 cm thick circular concrete roof was added to the silo. The horizontal radius of the roof was set to coincide with the outer radius of the silo, although based on the schematic picture of the shielded experimental configuration given in [4] and reproduced in Fig. 3 (left) the roof was slightly smaller in reality.

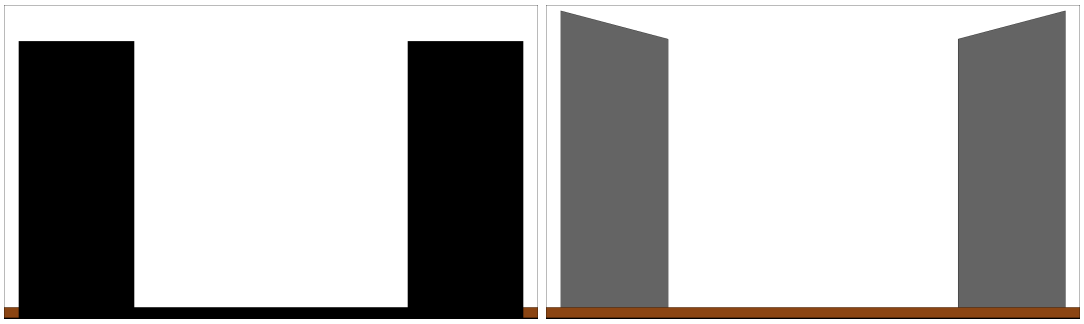

Figure 2. The two geometry models used for the source silo in the unshielded 150.5° cone skyshine experiment. ***Left****: Based on the MCNP model given in [2].* ***Right****: Based solely on the experiment description in [4]. Air is colored in white, whereas soil is brown and concrete is gray. Black indicates regions, where the photon tracks are immediately terminated.*

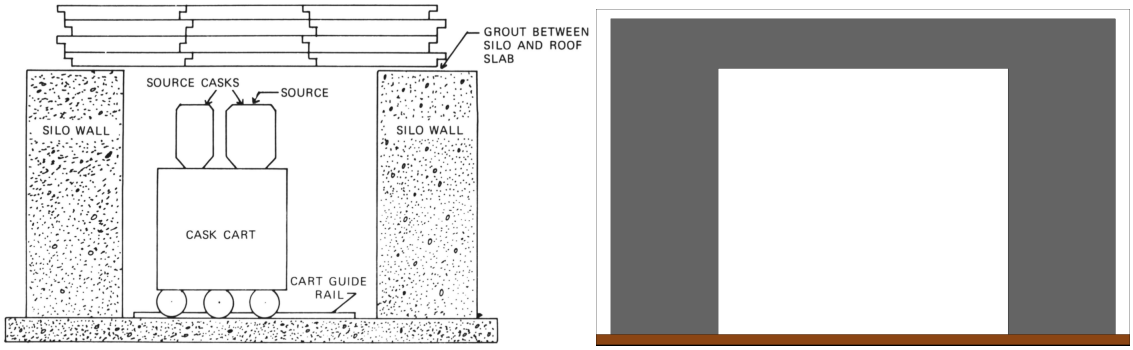

Figure 3. ***Left****: Schematic picture of the experimental arrangement for the* 42.8 cm *shielded skyshine experiment (from ref. [4]).* ***Right****: Vertical cut from Serpent geometry for the same experiment. The schematic picture is not drawn to scale, whereas the Serpent picture is.*

2.3.4 Experiment 3: 42.8 cm thick concrete roof

The geometry model for the third experiment was similar to that of the second experiment, with the only exception being the thickness of the roof, which was increased to 42.8 cm.

2.4 Results

The comparison between simulation and experiment was done using exposure rate constants instead of exposure rates, which vary by several orders of magnitude between the closest and furthest detectors. The experimental exposure rate constant Γ can be calculated based on the measured (or calculated) exposure rate $\dot{X}$, the distance from source to detector r and the activity of the source A:

$$\Gamma = \frac{\dot{X} r^2}{A} \tag{1}$$

Based on the measured exposure rates, values for Γ in micro Roentgen square meters per Curie hour ($\mu\mathrm{R\,m^2/(Ci\,h)}$) were calculated and reported for each measurement in the fifth column of tables I through III in [4]. For the simulations, the results were first converted to units of $\mu\mathrm{rad/(Ci\,h)}$. The MCNP estimates were converted by

$$\mathrm{MCNP}(\mu\mathrm{rad}/(\mathrm{h}\cdot\mathrm{Ci})) = \mathrm{MCNP}\left(\frac{\mathrm{MeV}}{\mathrm{cm}^3\cdot\mathrm{history}}\right)\cdot\left(1.899\cdot 10^{15}\,\frac{\mu\mathrm{rad}/(\mathrm{h}\cdot\mathrm{Ci})}{\mathrm{MeV}/(\mathrm{cm}^3\cdot\mathrm{history})}\right)\cdot 2.$$

Full derivation of the conversion factor is presented in Ref. [2]. The multiplication by the factor of two is not present in Ref. [2]. As approximately two photons are emitted in each decay of ^{60}Co, this multiplication is necessary, when comparing the detector estimates to the experimental results. The Serpent estimates were converted by

$$\text{Serpent}(\mu\text{rad}/(\text{h}\cdot\text{Ci})) = \frac{\text{Serpent}(\text{J}/\text{history})}{V(\text{cm}^3)} \cdot \left(1.185\cdot 10^{28}\,\frac{\mu\text{rad}/(\text{h}\cdot\text{Ci})}{\text{J}/(\text{cm}^3\cdot\text{history})}\right)\cdot 2,$$

where V is the detector volume and the multiplication by two is again due to approximately two photons being emitted in each decay of ^{60}Co. The µrad/(Ci h) values were then converted to µR/(Ci h) by using a conversion factor of 0.877 rad/R. Finally, the tallied results at each detector position were multiplied with the square of the distance of the detector from the source to obtain the Γ.

2.4.1 Experiment 1

In the MCNP calculation 151 million photon histories were simulated, whereas the number of histories was $5{\cdot}10^{10}$ in the Serpent calculation. Relative errors in the MCNP detector estimates were between 0.05 % and 0.21 %, and in the Serpent detector estimates between 0.030 % and 0.229 %. It is not beneficial to compare the relative errors between the codes as the detector types used by each code were crucially different. Moreover, weight-window based variance reduction was used in the MCNP calculations. The results of the simulations along with the experimental data are presented in Figure 4. The exposure rate constants are plotted as a function of Radius·Density to properly account for the variations in the air density during the measurements. The experimental data was taken from Table I of Ref. [4]. Relative differences between Serpent and MCNP results are presented in Figure 5 and they were calculated as

$$\text{Relative difference} = \frac{\text{Serpent} - \text{MCNP}}{\text{MCNP}}\cdot 100. \tag{2}$$

and the uncertainty of the relative difference was based on the total differential of the previous equation yielding

$$\Delta\text{Relative difference} = \frac{\text{MCNP}\times\Delta\text{Serpent} + \text{Serpent}\times\Delta\text{MCNP}}{\text{MCNP}\times\text{MCNP}}\cdot 100, \tag{3}$$

where Δ represents the absolute value of one sigma uncertainty in a certain result.

Agreement between Serpent and MCNP results is very good considering the statistical accuracy of the results. The differences between the codes stay inside 2 sigma uncertainties for all detector positions. Both Serpent and MCNP calculated values significantly underestimate the measured values for the three closest detectors. At the further detectors the agreement between calculated and experimental data is reasonable. The more realistic geometry model (input 2) performs noticeably better in the three closest detectors, but yields similar results to the basic model at the furthest detectors. It should be noted that the MCNP results reported in Fig. 4.6 of Ref. [2] have a much better agreement with the experimental data at the closest detectors and overestimate the results in the furthest detectors. The reasons for this difference are not known, but were not explained by code version or interaction data libraries: Ref. [8] shows results for the same experiment calculated with MCNP4C2 using the MCPLIB02 photon data library with a good agreement between MCNP results and measured data in the closest detectors. We could not obtain similar results with MCNP4C2 and the MCPLIB02 photon data library using the MCNP input included in [2]. The input model included in [2] might not be the final model used for the validation calculations for MCNP or there may be a difference in the conversion from rads to Roentgens between our simulations and those reported in [4] and [8].

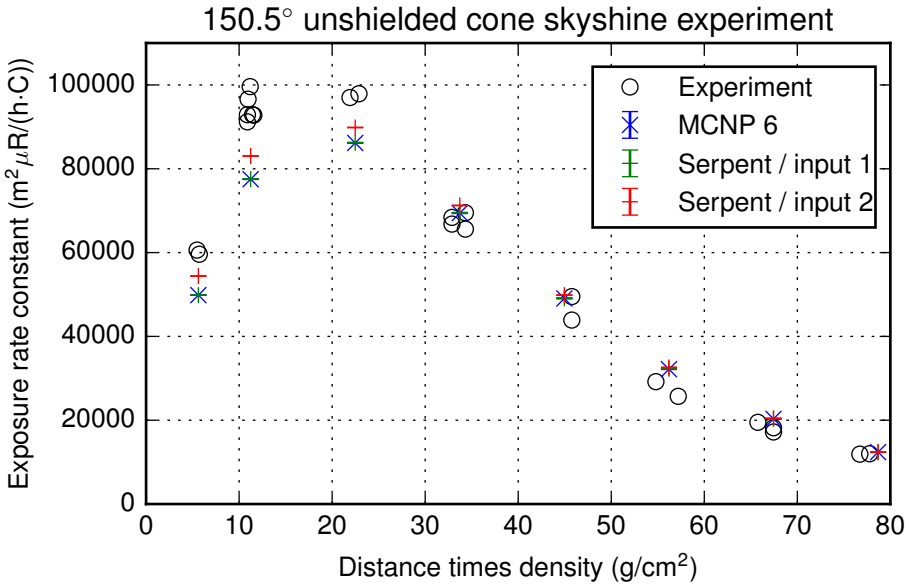

Figure 4. Results of the exposure rate measurements and simulations.

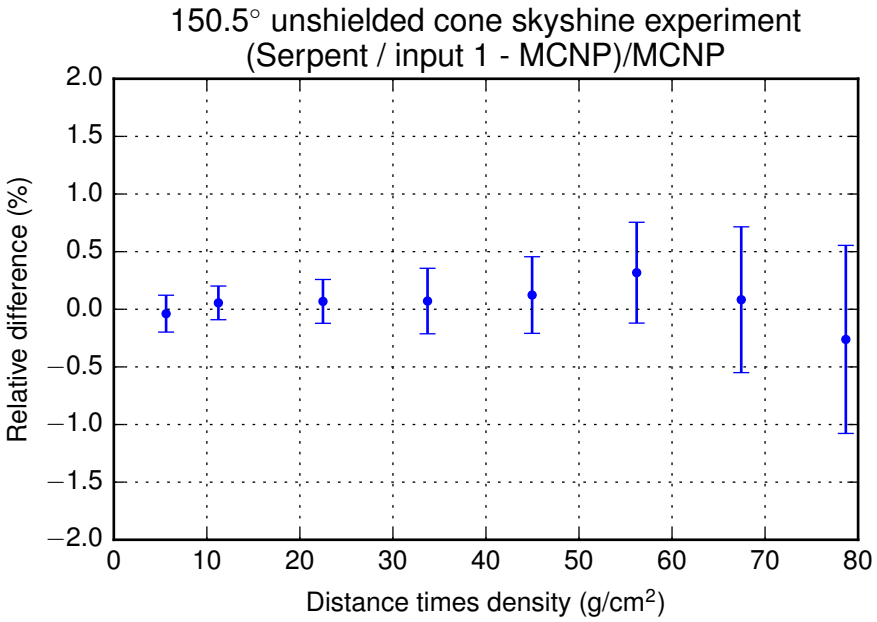

Figure 5. Relative differences in tallied dose rates between Serpent and MCNP results.

2.4.2 Experiment 2

The Serpent simulation for the second experiment used 5×10^{10} particle histories resulting in relative uncertainties between 0.05 % and 1 % in the dose rate tallies. The results of the simulation along with the experimental data are presented in Figure 6. The simulation yields 5–15 % larger exposure rates than the ones measured in the experiment, although the general trend in the measured exposure rates as a function of distance from the source is preserved well.

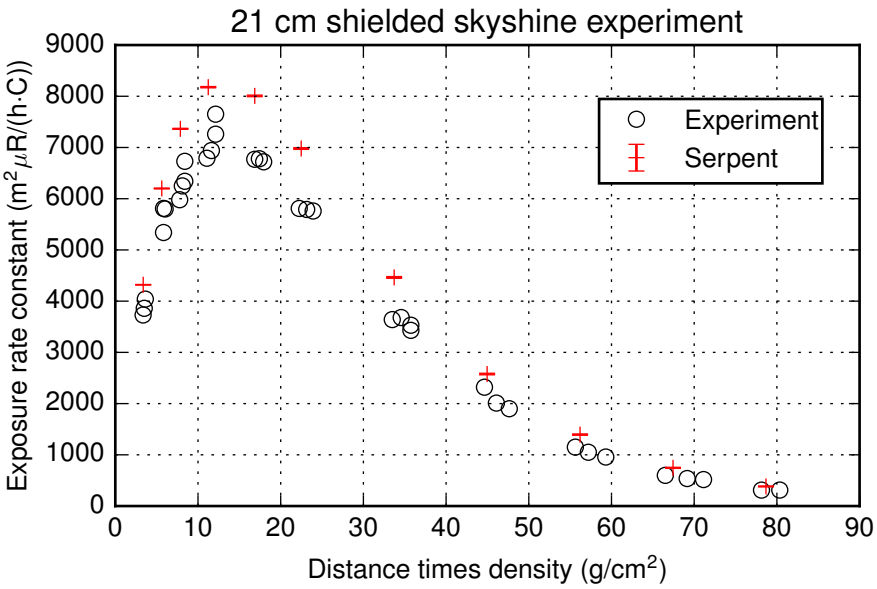

Figure 6. Results of the exposure rate measurements and simulations.

2.4.3 Experiment 3

The Serpent simulation for the third experiment used 1×10^{11} particle histories resulting in relative uncertainties between 0.1 % and 3 % in the dose rate tallies. The results of the simulation along with the experimental data are presented in Figure 7. The simulation results in higher exposure rates than was measured in the experiment similar to what was seen with experiment 2. However, the general trend in the measured exposure rates as a function of distance from the source is again preserved well.

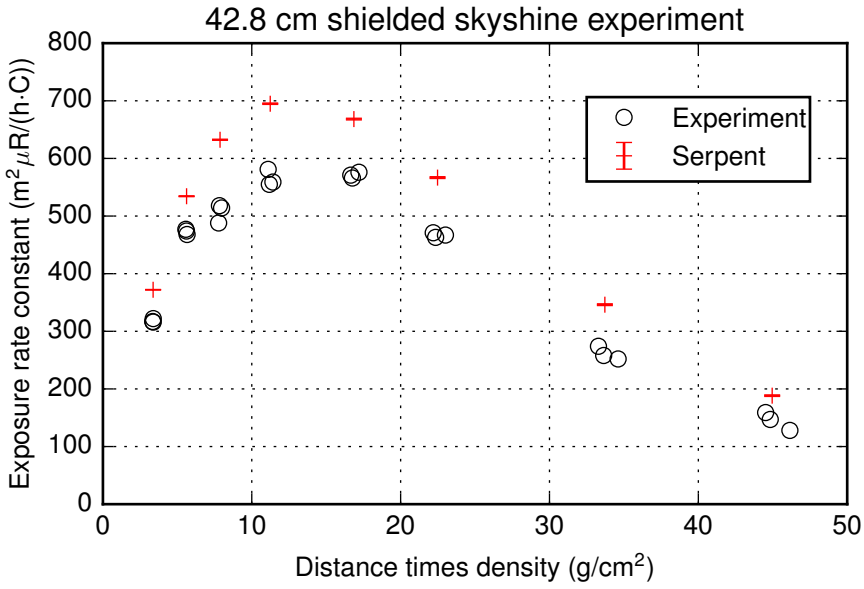

Figure 7. Results of the exposure rate measurements and simulations.

2.4.4 Additional calculations for the skyshine experiments

The results from experiments 2 and 3 suggest that the Serpent calculations underestimate the shielding effect of the concrete roof when compared with the experimental results. In order to investigate whether this underestimation is unique to Serpent, further calculations were made with Serpent and MCNP6 for a concrete shielded skyshine configuration based on the basic input of experiment 1. The input described in section 2.3.1 was modified by adding a 21 cm thick concrete roof on top of the silo similar to experiment 2. The dose rates were tallied with both codes at distances corresponding to the placement of detectors in experiment 2. Based on the results, relative differences between Serpent and MCNP6 were calculated similar to section 2.4.1.

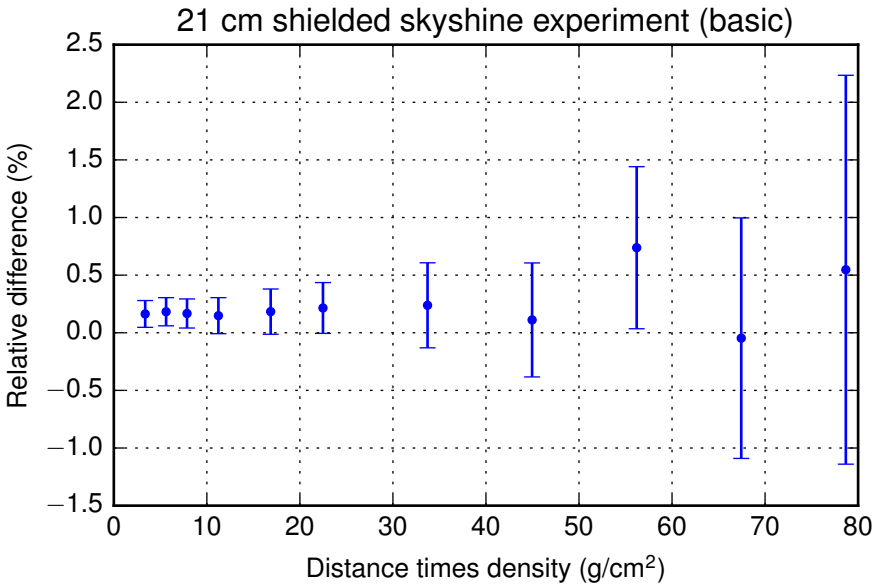

Figure 8. Relative differences in tallied dose rates between Serpent and MCNP results.

The relative difference between the two codes is shown in Figure 8. The photon dose rates calculated by the codes match quite well, however a small systematic difference can be inferred from the data with the Serpent simulation resulting in slightly higher dose rates. The good agreement between Serpent and MCNP both in this shielded model as well as the unshielded model (Fig. 5) leads us to conclude that Serpent does calculate the attenuation in the concrete shield correctly (according to the computational model) and the differences between the calculated results and experimental results for experiments 2 and 3 are due to differences between the computational model and the experiment.

Finally, a variation was applied to the density of the concrete in order to determine, whether the results from experiments 2 and 3 could be explained by uncertainties in the concrete dimensions, density or composition. The results from calculations using a concrete density of $2.25\,\mathrm{g/cm^3}$ instead of the nominal $2.13\,\mathrm{g/cm^3}$ reported in Ref. [4] are shown in three plots in Figure 9. The agreement between the calculated and experimental results was vastly improved for the shielded experiments and the results of the unshielded experiment were not adversely affected. This serves to show that the differences can be explained solely with the difference in the photon attenuation by the concrete structures. The increase in the concrete density cannot, however, be fully supported by the uncertainties reported in Ref. [4] as the required increase in density was approximately 5.6 % and the uncertainties in both the roof thickness and the

concrete density were approximately 1 %. The uncertainties in the concrete composition are more difficult to quantify as no composition was provided.

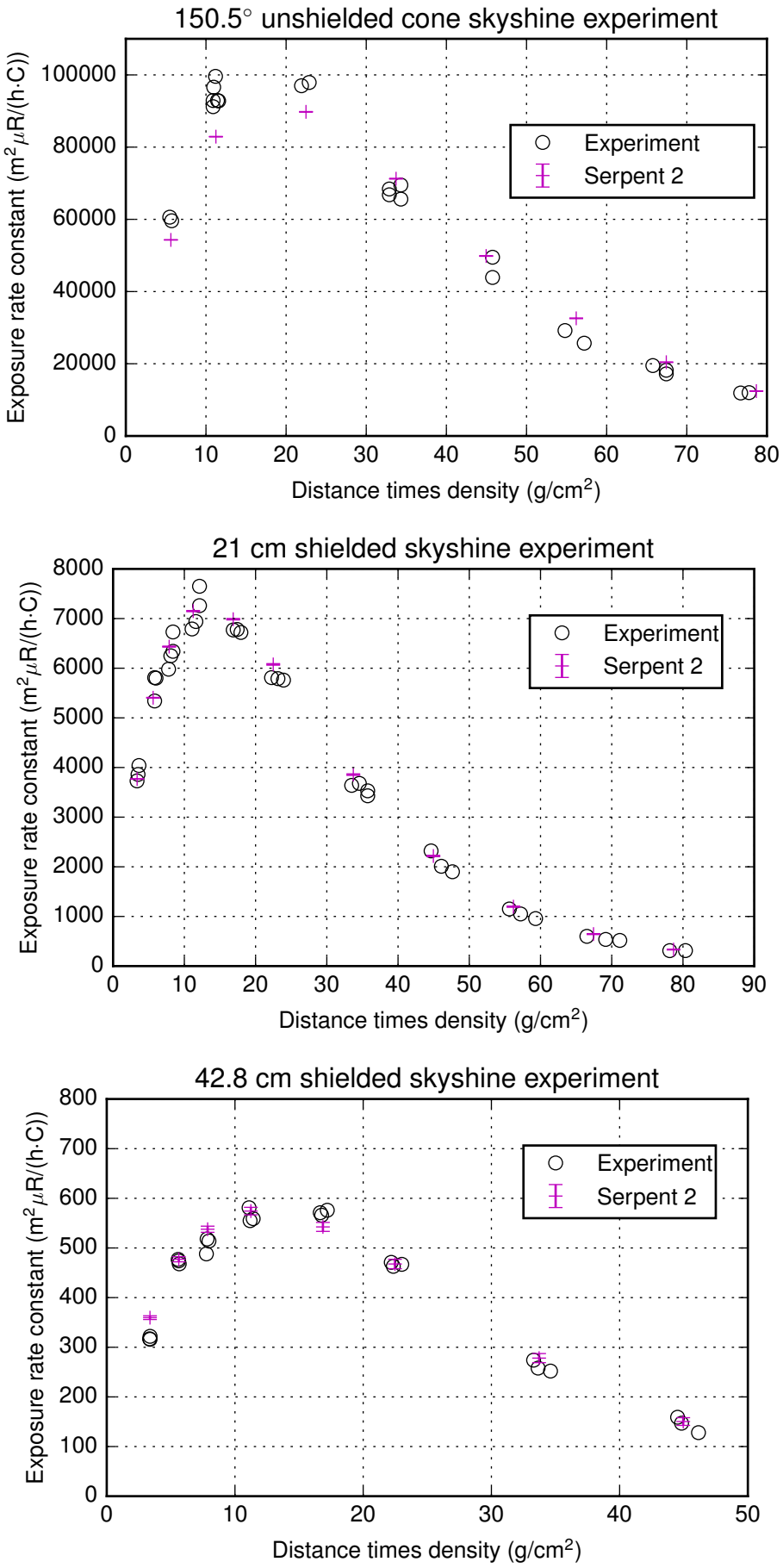

Figure 9. Serpent results for skyshine experiments using a concrete density of 2.25 g/cm^3.

3. Hupmobile TLD experiment

3.1 Problem description

This benchmark problem presented in Ref. [2] is based on the Hupmobile thermoluminescent dosimeter (TLD) experiments conducted at Lawrence Berkeley Laboratory between 1967 and 1969 [5, 6]. In the experiments, a gamma/x-ray point source was placed in air, one meter from one end of a teflon cylinder along its axis. Inside the cylinder on its axis were 17 LiF TLDs. One normalization TLD was also placed one meter beyond the source and two meters from the end of the teflon cylinder along its axis. The experimental arrangement is presented in Figure 10. The TLDs were used to register doses. In order to make the experimental data independent of source strength, the doses of the cylinder TLDs were divided by the dose of normalization TLD.

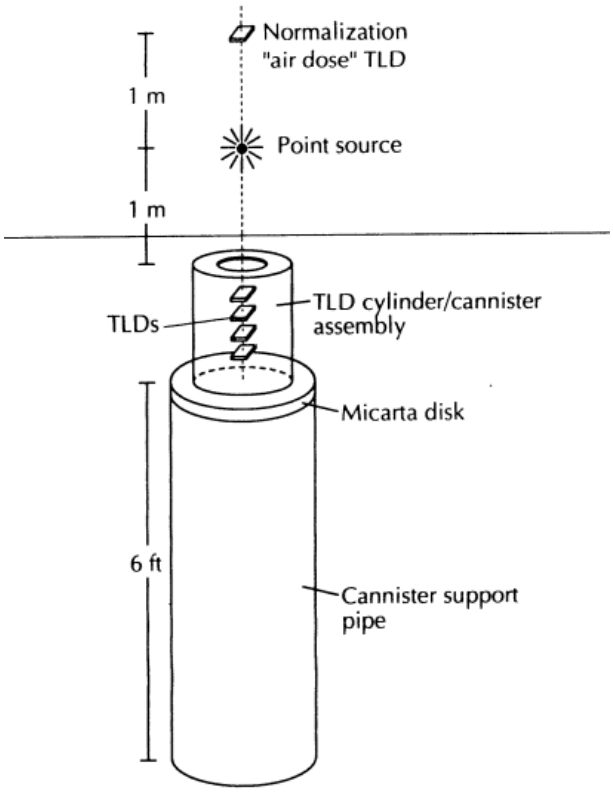

Figure 10. Experimental arrangement in the Hubmobile TLD experiments (Source: [2]).

The original technical reports [5, 6] were not found online so comparison with the measurement data was not possible. Therefore only one experiment with ^{137}Cs source was modelled with Serpent and the results were compared against MCNP6. Only the doses registered by the TLDs in the cylinder were calculated.

3.2 Serpent and MCNP models

Serpent model was build based on the MCNP model presented in Ref. [2], which also included an example MCNP input. The following describes how the MCNP model was built by the authors of Reference [2] and how it differs from the Serpent model.

The geometry was the same in both models and it was bounded by a 300 cm sphere centred at the origin. Other components of the geometry were placed parallel to the x-axis in the original MCNP model and parallel to the z-axis in the Serpent model. In the following description the orientation of the Serpent model is used. A teflon cylinder with a height of 30.48 cm and a radius of 13.97 cm was centred on the z-axis. This cylinder was sheathed by a cylindrical iron shell with the same height and wall thickness of 0.635 cm. The cylinder and the shell were capped by two iron disks which both had a radius of 14.605 cm. The disk closer to the source had a hole with a 6.985 cm radius cut from its center and it was 0.953 cm thick. The other disk had a thickness of 0.635 cm. The support stand and the micarta disk used in the experiment were not included in the geometry.

In Serpent the ^{137}Cs gamma source was modelled as an isotropic point source which emitted 0.661 MeV photons. The source was placed on the z-axis one meter from the end of the teflon cylinder. In the Serpent model source rate was set to 1 photon/s. In the MCNP model the point source was biased to emit a majority of photons into a cone subtended by the iron disk closer to the source. This biased sampling was used for variance reduction.

In the MCNP model 17 point flux estimators were placed inside the teflon cylinder on its axis. Their positions matched the positions of the TLD detectors used in the experiment. By modifying the flux estimates with an FM card, the energy deposited in unit volume per photon history MeV/(cm^3·history) was obtained.

In the Serpent model track length detectors and macroscopic heating cross section response function were used. Each of the detectors was defined using a cylinder with a radius of 1 cm and a height of 0.2 cm. The centre of each cylinder matched the position of the corresponding point flux estimator in MCNP. The output of the detectors was in units of J/history.

In the MCNP model variance reduction technique, based on assigning importances to the cells, was used in addition to the direction biased source. Thick-target bremsstrahlung approximation (TTB) was set on in the Serpent model and minimum mean distance for the collision flux estimator was set to $1{\cdot}10^6$.

3.3 Results

MCNP and Serpent detector estimates were converted to units of J/(cm^3·history) by multiplying the MCNP estimates by $1.60217662{\cdot}10^{-13}$ J/MeV and dividing the Serpent estimates by 0.62832 cm^3 (the volume of each detector cylinder). In the MCNP calculation $6.25{\cdot}10^7$ photon histories and in the Serpent calculation $2{\cdot}10^{11}$ photon histories were simulated. Relative errors in the MCNP detector estimates were between 0.19 % and 0.50 %, and in the Serpent detector estimates between 0.043 % and 0.238 %. The results of the simulations are presented in Figure 11. Relative differences between Serpent and MCNP results calculated with equation (2) are shown in Figure 12.

In general, agreement between Serpent and MCNP results is good. Some of the small differences in the estimated dose might be explained by the different types of detectors used in the Serpent and MCNP models. In MCNP point detectors were used but in Serpent track length detectors covering a finite volume around each corresponding MCNP point detector were used.

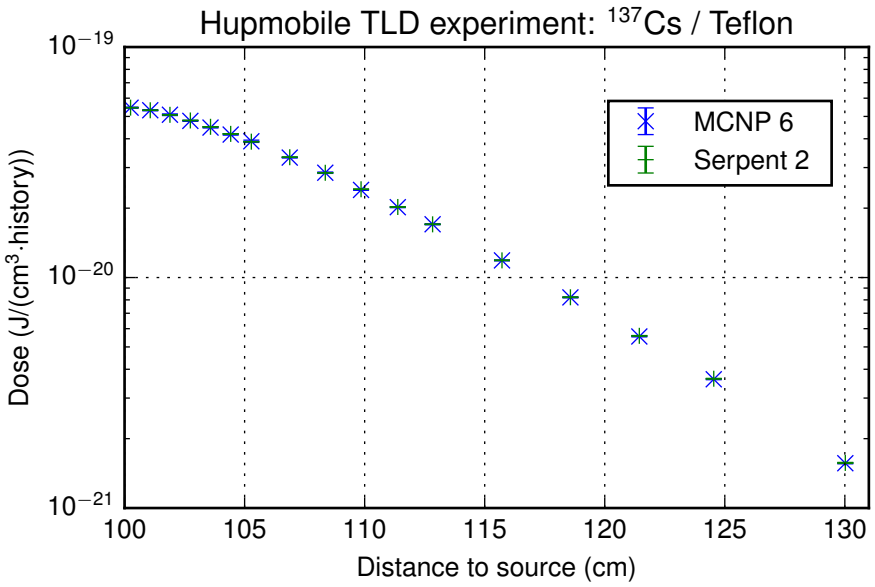

Figure 11. Results of the teflon dose rate simulations.

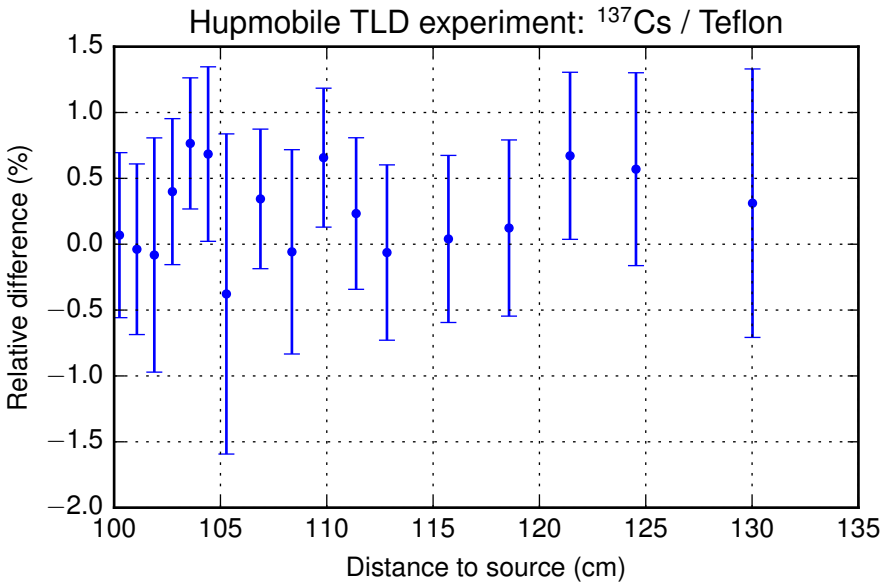

Figure 12. Relative differences between Serpent and MCNP results.

4. SINBAD benchmark experiments

SINDAB (Shielding Integral Benchmark Archive Database) is an electronic database for radiation shielding benchmark data [3]. The database is jointly developed and maintained by the OECD/NEA (Organization for Economic Cooperation and Development, Nuclear Energy Agency) Data Bank and ORNL/RSICC (Oak Ridge National Laboratory, Radiation Safety Informational Computational Center). The benchmark experiments are divided into three categories: reactor shielding (46 experiments), fusion neutronics shielding (31 experiments) and accelerator shielding (23 experiments). In the following, experiments with measured gamma radiation data are described briefly. However, experiments containing only measured nuclear heating (contribution from both neutrons and gammas) data and experiments from the accelerator shielding category are not included.

Winfrith Neutron-Gamma Ray Transport through Water/Steel Arrays (ASPIS)

Measured quantity:
Gamma dose rate
Gamma source:
From neutron transport calculation. Coupled neutron/gamma transport needed.
Additional information:
In the experiment a uranium fission plate driven by a thermal flux from NESTOR research reactor was used as a source. The plate was followed by an experimental configuration comprising several layers of steel and two water filled containers. Both neutron activation and gamma dose rates were measured in the experimental configuration. Example input files are not provided.

Radiation field parameters for pressure vessel monitoring in NRI LR-0 VVER-1000 reactor

Measured quantity:
Gamma spectrum
Gamma source:
From neutron transport calculation. Coupled neutron/gamma transport needed.
Additional information:
The source of radiation in the experiments was a VVER-1000 engineering benchmark assembly in the LR-0 experimental reactor. Neutron and photon spectra was measured over reactor pressure vessel thickness. Example input files are not provided.

Photon Leakage Spectra from Al, Ti, Fe, Cu, Zr, Pb, U238 Spheres

Measured quantity:
Gamma spectrum
Gamma source:
From neutron transport calculation. Coupled neutron/gamma transport needed.
Additional information:
In the experiments spherical and hemispherical samples of common structural materials were irradiated with a central 14 MeV D-T (Deuterium-Tritium) neutron source. Spectra and leakage of photons was measured. An example MCNP input file for the Fe sphere is provided.

Photon Spectra from H_2O, SiO_2 and NaCl

Measured quantity:
Gamma spectrum
Gamma source:
From neutron transport calculation. Coupled neutron/gamma transport needed.
Additional information:
The experimental arrangement was similar to the one used in the Photon Leakage Spectra from Al, Ti, Fe, Cu, Zr, Pb, U238 Spheres experiment. An example MCNP input file for the H_2O sphere is provided.

Baikal-1 Skyshine Benchmark Experiment

Measured quantity:
Gamma spectrum, gamma dose rate
Gamma source:
From neutron transport calculation. Coupled neutron/gamma transport needed.
Additional information:
In the experiments spatial energy distributions of air-scattered neutrons and photons from a research reactor in Baikal-1 research complex were measured. Example MCNP input files are provided for the calculation of photon dose rates. The dose rates were determined in two stages in the benchmark report: the contribution of secondary photons were determined by running a coupled neutron/gamma transport calculation and the contribution of primary photons of the core with a separate gamma transport calculation.

Aluminium Sphere (OKTAVIAN)

Measured quantity:
Gamma spectrum
Gamma source:
From neutron transport calculation. Coupled neutron/gamma transport needed.
Additional information:
In the experiments an aluminium sphere was irradiated with a central 14 MeV D-T neutron source. Leakage neutron and gamma spectra were measured. Several example MCNP input files with varying modelling accuracy are listed in the SINBAD abstract of the experiment but they are missing from the distribution available at VTT as are all the other files related to this experiment.

Silicon Sphere (OKTAVIAN)

Measured quantity:
Gamma spectrum
Gamma source:
From neutron transport calculation. Coupled neutron/gamma transport needed.
Additional information:
The experimental arrangement was similar to the one used in the Aluminium Sphere (OKTAVIAN) experiment. Several example MCNP input files with varying accuracy of modelling are provided. A 2D MCNP input with an explicit gamma source is provided. In the most detailed 3D MCNP model a separate source routine for the D-T neutron source is included.

Tungsten Sphere (OKTAVIAN)

Measured quantity:
Gamma spectrum
Gamma source:
From neutron transport calculation. Coupled neutron/gamma transport needed.
Additional information:
The experimental arrangement was similar to the one used in the Aluminium Sphere (OKTAVIAN) experiment. Several example MCNP input files with varying accuracy of modelling are provided. 1D and 2D MCNP inputs with explicit gamma sources are provided. In the most detailed 3D MCNP model a separate source routine for the D-T neutron source is included.

Manganese Sphere (OKTAVIAN)

Measured quantity:
Gamma spectrum
Gamma source:
From neutron transport calculation. Coupled neutron/gamma transport needed.
Additional information:
The experimental arrangement was similar to the one used in the Aluminium Sphere (OKTAVIAN) experiment. Two example MCNP input files are provided for the calculation of neutron leakage spectrum.

Collection of experimental data for fusion neutronics benchmark

Measured quantity:
Gamma spectrum, gamma dose rate
Gamma source:
From neutron transport calculation. Coupled neutron/gamma transport needed.
Additional information:
The collection includes experimental data from fusion benchmark experiments performed at the Japan D-T neutron source facility FNS at JAERI (Japan Atomic Energy Research Institute). Compilation of the data for SINBAD has not been carried out but original technical reports are included. In the experiments the gamma radiation is produced by neutron interactions.

FNS Integral Experiment on Graphite Cylindrical Assembly

Measured quantity:
Gamma dose rate
Gamma source:
From neutron transport calculation. Coupled neutron/gamma transport needed.
Additional information:
In the experiment a cylindrical graphite assembly was placed in front of a 14 MeV D-T neutron source. Neutron and gamma related responses were measured in several positions in the assembly. Example MCNP input files are provided for neutron transport calculations.

FNS Clean Experiment on Vanadium Cube

Measured quantity:
Gamma spectrum, gamma dose rate
Gamma source:
From neutron transport calculation. Coupled neutron/gamma transport needed.
Additional information:
In the experiment a vanadium cube was irradiated with a 14 MeV D-T neutron source. Neutron spectra, dosimetry reaction rates, gamma spectra and gamma heating rates were measured at three positions inside the assembly. Example MCNP input file with a separate source routine for D-T source is provided along with a simplified 1D MCNP input.

FNS Clean Experiment on Tungsten Cylindrical Assembly

Measured quantity:
Gamma spectrum, gamma dose rate
Gamma source:
From neutron transport calculation. Coupled neutron/gamma transport needed.
Additional information:
In the experiment a cylindrical tungsten assembly was irradiated with a 14 MeV D-T neutron source. Neutron spectra, dosimetry reaction rates, gamma spectra and gamma heating rates were measured at three positions inside the assembly. Example MCNP input file with a separate source routine for D-T source is provided along with a simplified 1D MCNP input.

FNS Radiation Skyshine with D-T Neutron Source

Measured quantity:
Gamma spectrum
Gamma source:
From neutron transport calculation. Coupled neutron/gamma transport needed.
Additional information:
In the experiment skyshine from a 14 MeV D-T neutron source was studied. Neutron dose rates, neutron spectra and gamma spectra were measured at distances up to 550 m from the source. Information on the response function and the efficiency of the detector used for the gamma spectrum measurements is not available so comparisons with gamma transport calculations are not possible. Example MCNP input are provided for neutron transport calculations.

FNG-ITER Dose Rate Experiment

Measured quantity:
Gamma dose rate
Gamma source:
Activated material compositions from neutron transport calculation. Decay source from compositions.
Additional information:
In the experiment a stainless steel/water assembly was irradiated with a 14 MeV D-T neutron source for a total of 18 hours in three days. One of measured quantities was dose rate in the center of the assembly after shut down from half an hour to more than three months of cooling time. In the benchmark report FISPACT(inventory code)/MCNP code system was used.

FNG/TUD Silicon Carbide (spectra measurements)

Measured quantity:
Gamma spectrum
Gamma source:
From neutron transport calculation. Coupled neutron/gamma transport needed.
Additional information:
In the experiment a silicon carbide benchmark assembly was irradiated with a 14 MeV D-T neutron source. Neutron and gamma spectrum were measured at four positions inside the assembly. Example MCNP input file with a separate source routine for D-T source is provided.

FNG Tungsten (integral)

Measured quantity:
Gamma dose rate
Gamma source:
From neutron transport calculation. Coupled neutron/gamma transport needed.
Additional information:
In the experiment a block of tungsten alloy was irradiated with a 14 MeV D-T neutron source. Neutron reaction rates and absorbed gamma doses were measured inside the block. Example MCNP input file with a separate source routine for D-T source is provided.

FNG/TUD Tungsten (spectra measurements)

Measured quantity:
Gamma spectrum
Gamma source:
From neutron transport calculation. Coupled neutron/gamma transport needed.
Additional information:
In the experiment a block of tungsten alloy was irradiated with a 14 MeV D-T neutron source. Neutron and gamma spectra were measured at four positions inside the assembly. Example MCNP input file with a separate source routine for D-T source is provided.

TUD Iron Slab Experiment

Measured quantity:
Gamma spectrum
Gamma source:
From neutron transport calculation. Coupled neutron/gamma transport needed.
Additional information:
In the experiment iron slab assemblies were irradiated with a 14 MeV D-T neutron source. Neutron and gamma spectra of the radiation which had penetrated the slabs were measured. Example MCNP input files is provided for neutron transport calculation.

ORNL 14-MeV Neutron SS/Borated Poly Slab

Measured quantity:
Gamma spectrum
Gamma source:
From neutron transport calculation. Coupled neutron/gamma transport needed.
Additional information:
In the experiment neutron and gamma spectra were measured behind stainless steel or stainless steel and borated polyethylene slabs which were irradiated with a 14 MeV D-T neutron source. Example input files are not provided.

MEPhI empty slits streaming experiment

Measured quantity:
Gamma spectrum
Gamma source:
From neutron transport calculation. Coupled neutron/gamma transport needed.
Additional information:
In the experiment iron shielding models with empty slits were irradiated with a 14 MeV D-T neutron source. Neutron reaction rates, heating rates, neutron and gamma spectra were measured. Example MCNP input is provided.

5. Conclusions

The validation of the photon physics routines in Serpent 2 were started by modelling several photon transport benchmark problems.

In the Kansas skyshine experiments, a good agreement was seen between Serpent 2.1.27 and MCNP6. However, the comparison to experimental data showed moderate differences in the three closest detectors for the unshielded skyshine experiment. It should be noted that the MCNP validation results presented in Ref. [2] and Ref. [8] showed a better agreement between calculated and experimental results in the three closest detectors for reasons that could not be identified. The calculations for the shielded experiments showed that the computational tools underestimated the source attenuation by the shielding concrete resulting in an overestimation of the exposure rates. Increasing the density of the concrete by approximately 5.6 % led to a good agreement between the calculated and the experimental results indicating that the differences could be solely due to the computational model for the concrete shield.

In the Hupmobile TLD experiment, good agreement was seen between the two codes with the differences being within 2 sigma uncertainty in 13 of the calculated 17 detector positions (76 %). Comparison to experimental data could not be done as the experimental data was not available in online sources.

The SINBAD database of shielding benchmarks was reviewed in order to identify experiments that can be used to further validate the photon transport capabilities of Serpent 2 in the future. 21 experiments with measured gamma radiation data were identified and summarised. Most of the SINBAD experiments are based on a known neutron source that generates photons through neutron interactions with various target materials, which means that the photon source needs to be generated through a neutron transport calculation. This requires, and can be used to validate, the coupled neutron/photon calculation mode that is being implemented in Serpent 2.

References

[1] T. Kaltiaisenaho. Implementing a photon physics model in Serpent 2. Master's thesis, Aalto University, School of Science, 2016.

[2] D. J. Whalen, D. E. Hollowell, and J. S. Hendricks. MCNP: Photon Benchmark Problems. Technical Report LA-12196, Los Alamos National Laboratory, 1991.

[3] I. Kodeli, E. Sartori, and B. Kirk. SINBAD – Shielding Benchmark Experiments – Status and Planned Activities. In Proceedings of the ANS 14th Biennial Topical Meeting of Radiation Protection and Shielding Division, Carlsbad, New Mexico (April 3-6, 2006).

[4] R. R. Nason, J. K. Shultis, and R. E. Faw. A Benchmark Gamma-Ray Skyshine Experiment. *Nuclear Science and Engineering*, 79:404–416, 1981.

[5] E. Goldberg, D. J. Groves, D. E. Jones, H. F. Luty, K. F. Petrock, G. A. Pohl, and D. H. White. Experiments to Test Validity of SORS-G Monte Carlo Code: I, Au-198 and Cs-137. Technical Report UCID-121, Lawrence Livermore National Laboratory, 1967.

[6] E. Goldberg, D. J. Groves, D. E. Jones, H. F. Luty, K. F. Petrock, G. A. Pohl, D. H. White, and R. Worley. Experiments to Test Validity of SORS-G Monte Carlo Code. Technical Report UCIR-368, Lawrence Livermore National Laboratory, 1969.

[7] R. J. McConn Jr., C. J. Gesh, R. T. Pagh, R. A. Rucker, and R. G. Williams III. Radiation portal monitor project, compendium of material composition data for radiation transport modeling. Technical Report PNNL-15870 Rev. 1, Pacific Northwest National Laboratory, 2011.

[8] R. D. Mosteller. Validation suites for mcnp. Technical Report LA-UR-02-0878, Los Alamos National Laboratory, 2002.